# Application of Compressed Sensing to $^{19}$F turbo spin echo chemical shift imaging

**T. C. Basse-Luesebrink[1,2], J. Beck[1], T. Kampf[1], A. Fischer[1,3], G. Weise[2], G. Stoll[2], and P. M. Jakob[1,3]**

[1]Experimental Physics 5, University of Wuerzburg, Wuerzburg, Bavaria, Germany, [2]Neurology, University of Wuerzburg, Wuerzburg, Bavaria, Germany, [3]Magnetic Resonance Bavaria, Wuerzburg, Bavaria, Germany

## Introduction

The application of compressed sensing (CS) to $^{19}$F steady-state free precession chemical shift imaging (ssfp-CSI) was recently introduced for fast acquisition of spatially resolved spectral $^{19}$F data (1,2). Turbo spin echo-based CSI (TSE-CSI) was previously used to allow an accelerated acquisition of multiple $^{19}$F markers (3,4). The current work focuses on combining CS with TSE-CSI to (A) increasingly accelerate the acquisition process; (B) take advantage of the long $T_2$ relaxation times of certain perfluorocarbon (PFC) $^{19}$F markers; and (C) retain the ability of CSI to distinguish between different $^{19}$F markers.

## Encoding scheme

For encoding, the k-space was divided in circular segments containing the same number of points. The segment number was the number of echoes (number of echoes = turbo factor (TF)). Since, in a TSE sequence, the signal intensity for later echoes is decreased by $T_2$ decay, the segments were sorted from inside to outside according to the echo number (Fig.1A).

For acquisition of the undersampled data, the number of points per segment was decreased by the acceleration factor (af). The size of the central segment containing the first echoes was reduced to fit the decreased number of points per segment. This enabled a dense sampling of the inner k-space, which is preferable for CS (1). The points were randomly distributed in all other segments (Fig.1B).

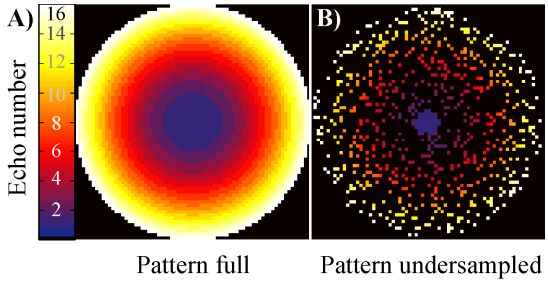


Fig.1 A) Acquisition scheme for the TSE-CSI sequence (TF = 16). B) Undersampling pattern for a TSE-CSI sequence (TF = 16, af = 6). The k-space center is fully sampled using the first echo.

## Materials and Methods

The TSE-CSI sequence was implemented on a 7T small animal scanner. As described in (1), a C57/BL6-mouse with two focal cerebral ischemia induced by photothrombosis served as *ex vivo* phantom. The animal contained two PFC emulsions with different core compounds (PFC1: perfluoro-15-crown-5-ether; PFC2: perfluoro-polyethelene-oxide). The spectral separation of the main resonance peaks is approximately 0.8 ppm (~230 Hz at 7T).

A single mouse brain slice was imaged using the TSE-CSI sequence (Echo time/ acquisition time/ repetition time = 18.6/12.9/2000ms; spectral points = 64; spectral bandwidth: 5000Hz; matrix size = 72x72; field-of-view = 30x30mm$^2$; slice thickness = 2mm; TF = 16). Additionally undersampled data with af = 6 were acquired with the TSE-CSI sequence. CS reconstructions were performed using a CS algorithm that applied strict data consistency and only one sparsity constraint as described in (1,2). For comparison, TSE-CSI experiments with a smaller matrix size were performed as well as experiments acquired in a pseudo radial fashion (22 spokes) with approximately the same measurement time as the undersampled experiment.

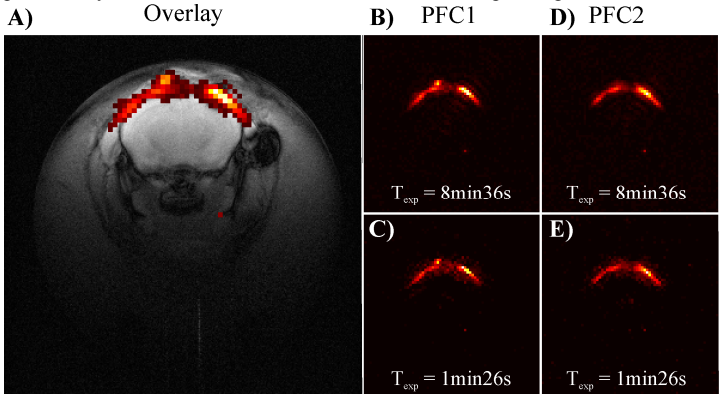


Fig.2) Comparison of fully sampled data with CS-reconstructed data. A) Overlay image showing that the PFC marker was accumulated under the skin. B) Fully sampled image at the resonance peak of the PFC1 maker (TF = 16). C) CS-reconstructed data (TF = 16, af = 6) of the resonance peak of the PFC1 compound. D-E) Analog to B-C for the PFC2 compound.

## Results

Fig.2 compares fully sampled data with undersampled, CS-reconstructed data. In Fig.2A, the fluorine data is presented in the anatomical context of the proton background data. Fig.2C-E shows that for both resonance lines, the undersampled data could be reconstructed using CS. This resulted in similar image quality as the fully sampled references. Fig.3 compares different acquisition strategies using TF = 16 and af = 6. The CS-reconstructed data (Fig.3D) provides a higher resolution than the low-resolved, zerofilled data acquired with the smaller matrix size (Fig.3A), the pseudo radial data (Fig.3B), and the random undersampled data (Fig.3C). Additionally, the zerofilled data suffers from Gibbs ringing (Fig.3A), streaking artifacts can be seen in the pseudo radial data (Fig.3B), and in-coherent artifacts are present in the random undersampled data (Fig.3C). The in-coherent artifacts were removed by the CS reconstruction; however, a slight "blooming" effect around the signal is visible (Fig.3D).

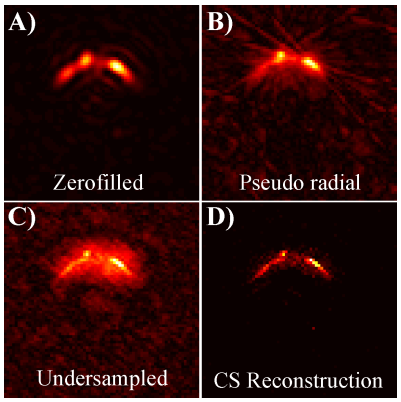


Fig.3) Comparison of different acquisition strategies. A) Zerofilled data (TF = 16, af = 6). B) Pseudo radial data (TF = 16, 22 spokes ~ af = 6). C) Undersampled data (TF = 16, af = 6). D) Same data as in C but CS-reconstructed.

## Discussion and Conclusion

CS was able to reconstruct undersampled data acquired with a TSE-CSI sequence using 2D centric encoding up to af = 6. This enabled fast acquisition of spectral as well as spatial information. Additionally, the distinction between multiple PFC markers could be preserved when TSE-CSI was undersampled and subsequently CS-reconstructed. Compared to other undersampling strategies, the CS-reconstructed data was superior in terms of resolution. The main limitation in the application of CS to $^{19}$F CSI/MRI is the SNR necessary for proper CS reconstructions (1). However, in $^{19}$F applications, with sufficient SNR, CS has the potential to significantly decrease the experiment time. Future application of CS to 3D TSE-CSI should allow acquisition of spatial and spectral $^{19}$F information in reasonable measurement time and with relatively high spatial resolution.

## References

[1] T. Kampf et al., J. Magn. Reson. (2010), doi:10.1016/j.jmr.2010.09.006
[2] A. Fischer et al., Proc. Intl. Soc. Mag. Reson. Med. 17 (2009) , p. 3154
[3] M. Yildirim et al., Proc. Intl. Soc. Mag. Reson. Med. 16 (2008) , p. 3257
[4] R. Lamerichs et al., Proc. Intl. Soc. Mag. Reson. Med. 17 (2009) , p. 617

## Acknowledgements

This work was supported by the DFG SFB 630 (C2); SFB 688 (B1,B5,Z2); the Bavarian Ministry of Economic Affairs, Infrastructure, Transport and Technology; and the IZKF Würzburg project F-25.